Recast layer removal of WEDMed surface by wire electrochemical finishing

Hongwei Pan (panhw122@nuaa.edu.cn)
Nanjing University of Aeronautics and Astronautics
Zhidong Liu
Xinsong Chen
Xiyuan Yin

Research Article

Keywords: WEDM, Multi-pass, Surface roughness, Recast layer, Microhardness

Posted Date: June 23rd, 2022

DOI: https://doi.org/10.21203/rs.3.rs-1737245/v1

Recast layer removal of WEDMed surface by wire electrochemical finishing

Hongwei Pan[1], Zhidong Liu[1*], Xinsong Chen[1] and Xiyuan Yin[1]

[1]College of Mechanical and Electrical Engineering, Nanjing University of Aeronautics and Astronautics, No.29, Yudao Str., Nanjing, 210016, Jiangsu, China.

*Corresponding author. E-mail: liutim@nuaa.edu.cn;

Abstract

To eliminate the recast layer on the surface machined by multi-pass wire electrical discharge machining (WEDM), hence improving the surface integrity, the present paper proposed and investigated a new combined machining process of performing wire electrochemical machining (WECM) after multi-pass WEDM on the same machine tool by utilizing the slight conductivity of the compound working fluid. A theoretical model based on the electric double layer and Faraday's law of electrolysis was established to calculate the wire feed rate for WECM finishing. Due to the exclusive film protection of the compound working fluid, the theoretical model was modified according to the experimental results under different electrolyte concentrations. Afterward, the optimized model was applied to guide the experiments of the combined process. An electrolyte concentration of 1:5 was used to facilitate the electrochemical reaction. The experimental results showed that the remaining recast layer after multi-pass WEDM could be completely removed at a wire feed rate of 10 μm/s, and a fine surface finish could be obtained. In addition, the surface roughness of the machined part was improved from 1.458 μm Ra to 0.683 μm Ra.

Keywords: WEDM, Multi-pass, Surface roughness, Recast layer, Microhardness

1 Introduction

The recent years have seen significant progress in increasing the machining rate and decreasing tool electrode wear of wire electrical discharge machining (WEDM) [1, 2]. However, surface and subsurface damages induced by its nature electro-thermal removal process severely confine the application of WEDM in aviation, aerospace, and other areas with high criteria for surface integrity [3]. After the spark discharge, the molten debris not expelled out of the machining gap timely will be rapidly cooled by the dielectric fluid. Then they will re-solidify and deposit and generally form a porous and crakced recast layer on the machined surface [4]. The recast layer is unavoidable and detrimental in WEDM since surface quality degradation directly endangers the fatigue strength and service life of the machined part [5].

Although the recast layer thickness can be reduced by the multi-pass WEDM, the material removal mechanism of the subsequent passes (trim cutting) still relies on thermal energy produced by electrical discharges, identical to the main cutting. Therefore, the recast layer cannot be completely removed by simply increasing the number of passes. Singh et al. [6] investigated the effect of pass number on the surface quality during machining of MWCNT alumina composites in WEDM. They found that after five passes, a recast layer with a thickness of about 2.1 µm was observed.

The non-contact wire electrochemical machining (WECM) has been extensively employed in manufacturing like WEDM but shows a different material removal mechanism from that of WEDM. WECM relies on the mechanism of anode electrochemical dissolution at the atomic level to remove material, with such advantages as no recast layer, residual stress, or microcrack on the machined surface [7]. Kurita et al. [8] developed EDM and ECM/ECM lapping complex machining technology to smooth the EDM surface, where ECM finishing was carried out by shifting from an EDM to an ECM power supply. The experiments showed that the EDM surface roughness could be improved to 0.06 µm Ra by ECM lapping. Nguyen et al. [9] proposed a unique hybrid machining in which the micro-EDM and micro-ECM were conducted simultaneously in low-resistivity deionized water. The research revealed a conversion of material removal mechanism from mere micro-EDM to hybrid micro-EDM/ECM at a low feed rate. As a result, greater surface quality and dimensional accuracy could be obtained during fabricating micro-features. Due to high-speed wire electrical discharge machining (HSWEDM), little research has been available on recast layer removal by incorporating other machining methods on the same machine tool.

To take full advantage of WEDM and WECM, this work develops a new machining technique combining multi-pass WEDM and WECM. First, an optimized multi-pass WEDM for shaping and semi-finishing is carried out to thin the recast layer as much as possible. Second, by utilizing the silghtly conductive JR1A compound working fluid widely used in HSWEDM as an electrolyte, WECM finishing is conducted to eliminate the remaining recast layer. Hence,

the sequential combination of WEDM and WECM can be performed on the same machine tool with a consistent power supply and machining fluid.

2 Experimental setup and approach

2.1 Experimental setup

This study applied the high-speed wire electrical discharge machine with the sophisticated multi-pass cutting function. Fig. 1 shows the photographic view of the experimental setup. Cr12 steel with a thickness of 40 mm was used as the work-piece, and molybdenum wire with a diameter of 0.18 mm was utilized as the wire electrode. The experimental conditions are listed in Table 1.

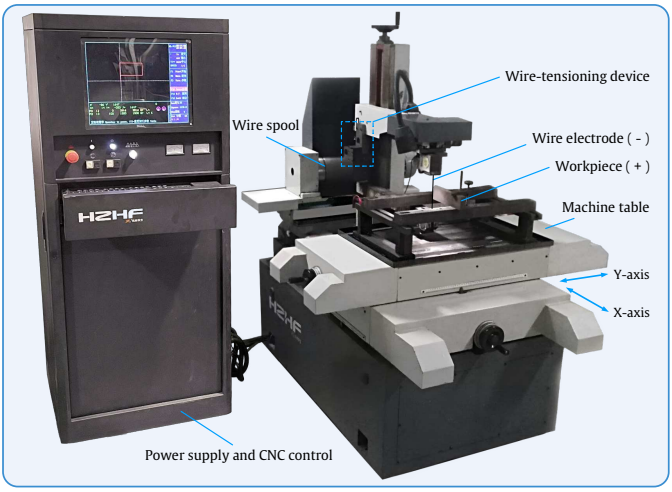

Fig. 1: Photograph of experimental setup

Table 1: Experimental conditions

Items	Conditions
Wire electrode	Molybdenum, diameter: φ0.18 mm
Work-piece	Cr12, thickness: 40 mm
Dielectric fluid	Compound working fluid, JR1A

2.2 WECM finishing approach

After main cutting with WEDM, the erosion debris is non-uniformly suspended in the narrow machining gap, causing unfavorable flushing conditions of the

electrolyte if performing WECM right after the main cutting. Moreover, the recast layer formed by the main cutting, especially that at high pulse energy, is usually discontinuous, thick, and varying [10]. Consequently, it is impossible to eliminate the recast layer by applying WECM finishing straightforwardly after the main cutting. Nevertheless, the recast layer could be dramatically reduced by utilizing the multi-pass WEDM strategy [11]. Furthermore, the continuousness and uniformity of the recast layer can be under effective controlled, beneficial for the successive WECM finishing. The schematic of the combined machining process of multi-pass WEDM and WECM is shown in Fig. 2. First, the optimized multi-pass WEDM process (one main cutting followed by two trim cutting) was carried out to diminish the thickness and distribution status of the recast layer. Second, the wire electrode was moved in the direction away from the desired surface by a certain distance, ensuring the WECM process without spark discharge.

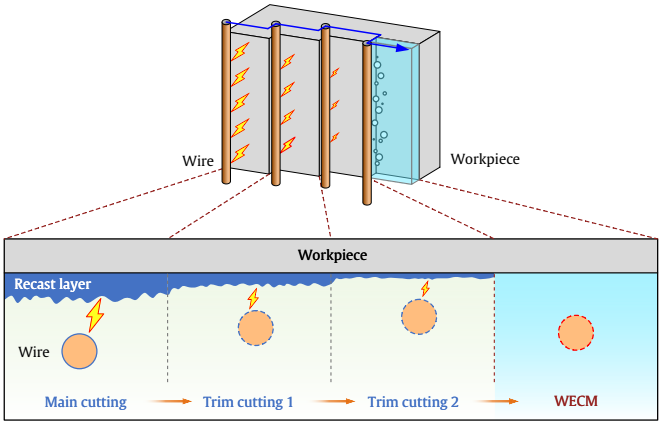

Fig. 2: Schematic of wire passes for multi-pass WEDM and WECM

Table 2: Optimized machining parameters for three-pass WEDM

Wire pass	Pulse width (μs)	Duty ratio	Current (A)	Wire traveling speed (m/s)	Offset (mm)	Wire feed rate (μm/s)
MC	40	1:5	4	12.0	0.000	50
TC1	10	1:8	2	7.2	0.040	100
TC2	3	1:10	1	4.8	0.020	80

Under the experimental conditions of this study, the preliminary multi-pass WEDM experiment was carried out using optimized parameters listed in Table 2. The machining energy was reduced gradually with every successive pass to form minimal craters and debris on the machined surface, thus improving the surface quality. After main cutting (MC), the offset values of the wire electrode towards the desired surface for the first (TC1) and second trim cutting (TC2)

were 0.040 mm and 0.020 mm, respectively. The average recast layer thickness after three passes could be controlled within 10 µm. Moreover, the unevenness of the recast layer was significantly lessened since a majority of the irregular re-solidified globules were removed, making it feasible for the consecutive WECM finishing.

The initial distance between the wire electrode and the desired surface after three-pass WEDM was about 0.005 mm, as detected from previous experiments. In order to avoid spark discharge between the work-piece and wire electrode during electrochemical dissolution, the wire electrode must be moved in the direction away from the desired surface by a certain distance [12]. This study carried out WECM finishing in the narrow machining gap generated by the previous three-pass WEDM. Therefore, the reverse offset of the wire electrode in the gap was considerably limited. To simplify the establishment and analysis of the model for WECM finishing, the reverse offset of the wire electrode after three-pass WEDM was set to be 0.030 mm according to the gap width and the previous offsets in two trim cutting. After the wire electrode moved by 0.030 mm in the direction away from the desired surface, a suitable machining gap for WECM was obtained since no spark discharge occurred during WECM. Fig. 3 shows the inter-electrode voltage-current waveform sampled during WECM with the reverse offset of 0.030 mm after three-pass WEDM. As can be seen, only an electrolytic reaction was found between two electrodes without the generation of spark discharge. The average current of the WECM process is 0.3 A.

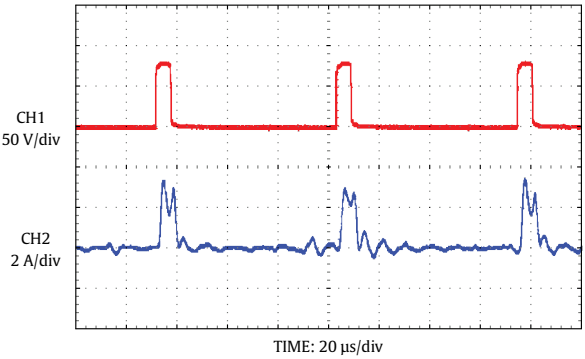

Fig. 3: Voltage-current waveform sampled during WECM

3 Model development to identify the wire feed rate

3.1 Establishment of WECM model

As WECM is an anodic dissolution process, the material removal is governed by Faraday's law [13],

$$m = \frac{M}{zF}Q = e_a Q \tag{1}$$

where, m is the mass of material removed from the anode, M is the molar mass of the substance, z is the valency of ions of the anode material, F is Faraday's constant, Q is the total charge involved in the reaction, and e_a is the electrochemical equivalent.

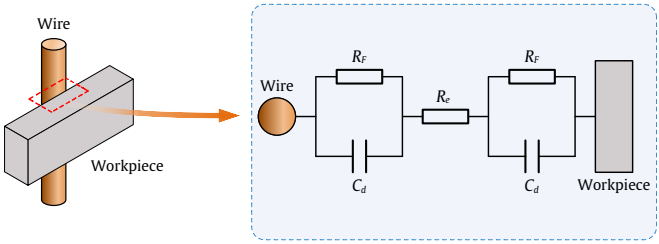

Fig. 4: Equivalent double layer circuit model during WECM

Fig. 4 shows the equivalent circuit model for the generated double layer during WECM [14]. In this model, double layer capacitance C_d remains parallel with the faradic reaction impedance R_F. The total double layer circuit constitutes two of these types of circuits, one for the cathode and another for the anode. These two circuits remain in series with the resistance of the electrolyte R_e, between the cathode and the anode. According to the circuit, the total equivalent resistance of the double layer R_{dl} can be calculated:

$$R_{dl} = R_e + \frac{2R_{cd}R_F}{R_{cd} + R_F} \tag{2}$$

where, R_{cd} is the impedance of the double layer capacitance. Based on the Gouy-Chapman-Stern model, R_{cd} can be expressed as:

$$R_{cd} = \frac{\delta}{fA\varepsilon_r\varepsilon_0} \tag{3}$$

where, δ is the thickness of Stern layer, f is the applied frequency, A is the area of machining, ε_r is the relative dielectric constant of electrolyte, ε_0 is the dielectric constant of the vacuum. In this study, the extremely large applied

frequency f enables the value of R_{cd} to be neglected, resulting in the approximate equivalence of the total equivalent resistance of the double layer R_{dl} to the electrolyte resistance R_e.

The schematic diagram of calculating R_e is illustrated in Fig. 5. The inter-electrode Cartesian coordinate system has been established, in which X-axis pointed to the wire feed direction, and Y-axis was along the direction away from the machined surface. In this study, the initial distance after three-pass WEDM between wire electrode and work-piece was denoted as d_i. Before WECM finishing, the wire electrode needed to be moved away from the machined surface by a distance of d_o. Then, the distance between any point $(x,\ y)$ on the wire electrode surface and the work-piece surface in the side inter-electrode gap can be expressed as:

$$d = d_i + d_o + r - \sqrt{r^2 - x^2} \tag{4}$$

where, r is the radius of the wire electrode.

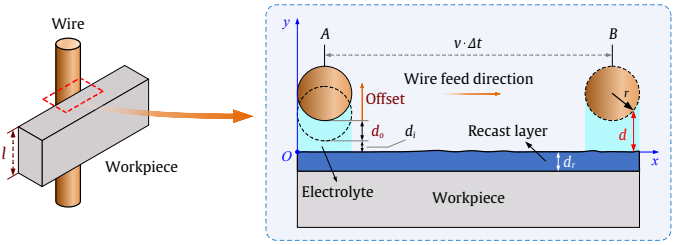

Fig. 5: Schematic diagram of the inter-electrode gap

Therefore, the resistance of the electrolyte can be calculated as:

$$R_e = \int_0^{2r} \frac{1}{\kappa dl} dx \tag{5}$$

where, κ is the conductivity of the electrolyte, and l is the thickness of the work-piece.

Knowing the resistance for current flowing in the machining zone, the total charges Q involved in the reaction can be calculated as:

$$Q = \frac{U}{R_e} \cdot t_e = \frac{U}{R_e} \cdot t \cdot \frac{t_{on} - \tau}{T} = \frac{Ut(D_r - \tau f)}{R_e} \tag{6}$$

where, U is the input pulse voltage, t_e is the electrolytic time, t is the machining time, t_{on} is the pulse duration, τ is the double layer charging time, T is the pulse period, and $D_r = t_{on}/T$ is the duty ratio. The double layer charging

time constant τ can be represented as:

$$\tau = \rho C_d \delta_{sg} \tag{7}$$

where, ρ is the resistivity of electrolyte, and δ_{sg} is the side inter-electrode gap.

On this basis, Eq. (1) can be re-written as:

$$m = e_a \cdot \frac{Ut(D_r - \tau f)}{R_e} \tag{8}$$

As shown in Fig. 5, when the wire electrode moves from positions A to B during the time Δt, the volume of materials dissolved on the work-piece is:

$$m = d_r(v\Delta t + 2r)l\rho_a \tag{9}$$

where d_r is the thickness of the recast layer, v is the wire feed rate, and ρ_a is the density of anode material.

From Eqs. (8) and (9), Eq. (10) can be obtained:

$$e_a \cdot \frac{Ut(D_r - \tau f)}{R_e} = d_r(v\Delta t + 2r)l\rho_a \tag{10}$$

Given that the machining time t is long enough in real-world machining, the dissolved thickness of the recast layer can be written as:

$$d_r = \frac{e_a U(D_r - \tau f)}{vl\rho_a R_e} \tag{11}$$

3.2 Optimization of WECM model

Through the aforementioned WECM model, the theoretical relationship between the main factors was established, namely the recast layer thickness, the electrolyte conductivity, the wire electrode offset, and the corresponding wire feed rate. Knowing the electrolyte conductivity and the wire electrode offset, the desired wire feed rate for electrolytic removal of the recast layer with a specific thickness can be calculated according to the theoretical model. However, the compound working fluid used in this study represented quite a complicated ingredient [15], in which the oily substance and rust inhibitor adsorbed on the electrode surface, forming a continuous and dense protective film. As the machining proceeded, the protective effect of the film increased, leading to a conversion of the electrode surface from activation dissolution to passivation. The formation of the protective film is shown in Fig. 6. With the improved concentration of the working fluid, the compactness and thickness of the adsorbent film on the electrode surface were enhanced, resulting in a less actual dissolution volume than the theoretical value while utilizing the compound working fluid as the electrolyte for WECM. The theoretical dissolution

volume d_t without considering the influence of the double layer and protective film can be simplified as:

$$d_r = \frac{e_a U D_r}{v l \rho_a R_e} \tag{12}$$

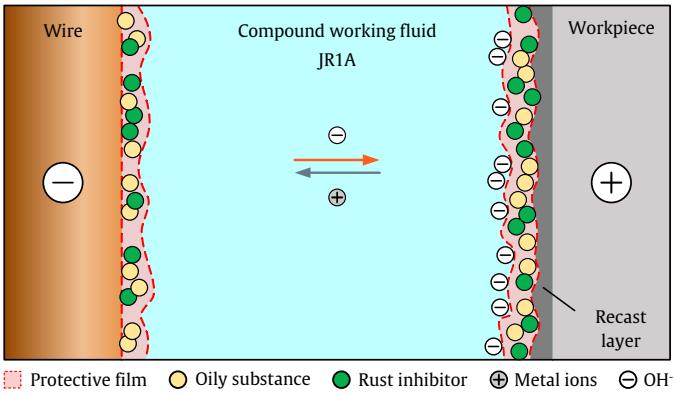

Fig. 6: Diagram of protective film on the electrode surface

While conducting electrolytic finishing using compound working fluid, the formation of the protective film was closely related to the concentration of working fluid. Table 3 lists the electrical conductivity of the compound working fluid measured at different concentrations. To optimize the compound working fluid-based WECM model, the deviation between actual and theoretical dissolution volume under different concentrations was investigated in this paper by conducting experiments. Afterward, the electrolytic model was revised by curve fitting technique to identify the relationship between the actual and theoretical dissolution volume. After performing a three-pass WEDM with the parameters listed in Table 2, WECM experiments at different concentrations were carried out, respectively, utilizing the experimental parameters shown in Table 4. The actual dissolution volume, denoted as thickness, was obtained by a micrometer from the average of three measurements. The experimental results are shown in Fig. 7.

Table 3: Electrolyte conductivity at different concentrations

Concentration of JR1A	Electrolyte conductivity (μS/cm)
1:20	3.89
1:15	4.79
1:10	6.18
1:5	10.63

Table 4: Electrolyte conductivity at different concentrations

Pulse width (μs)	Duty ratio	Wire traveling speed (m/s)	Offset (mm)	Wire feed rate (μm/s)
10	1:6	2.4	0.030	40
10	1:6	2.4	0.030	30
10	1:6	2.4	0.030	20
10	1:6	2.4	0.030	10

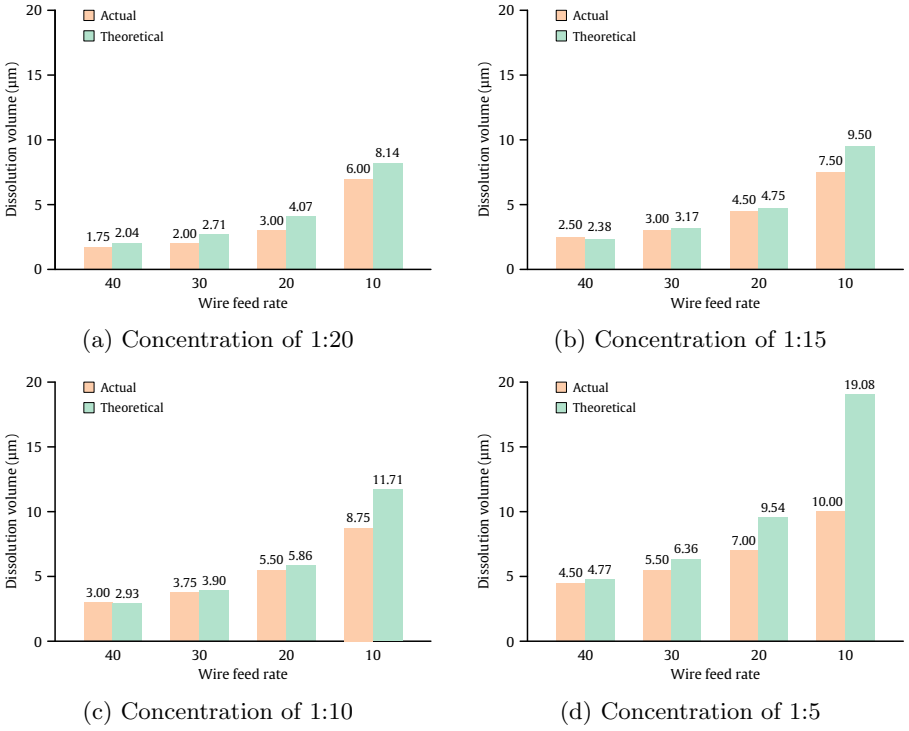

(a) Concentration of 1:20

(b) Concentration of 1:15

(c) Concentration of 1:10

(d) Concentration of 1:5

Fig. 7: Dissolution volume at different concentrations of compound working fluid

According to the experimental results, the fitting curves of the theoretical and actual dissolution volume at different concentrations of compound working fluid were plotted, as shown in Fig. 8. The fitting curves revealed that the actual dissolution volume (d_a) was linearly correlated to the theoretical value (d_t) at the same concentration of compound working fluid. On this basis, the optimized model could be used to identify the desired wire feed rate for WECM finishing after multi-pass WEDM.

As can be seen in Fig. 8, at the same electrolyte concentration, the actual dissolution volume increased as the wire feed rate decreased because a low wire feed rate prolonged the electrochemical reaction and thus resulted in

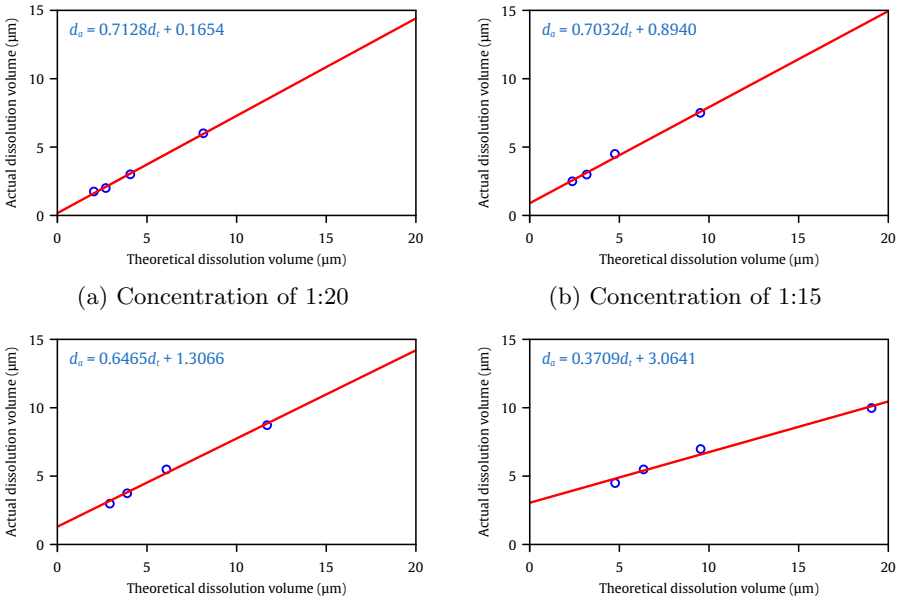

(a) Concentration of 1:20

(b) Concentration of 1:15

(c) Concentration of 1:10

(d) Concentration of 1:5

Fig. 8: Dissolution volume at different concentrations of compound working fluid

more dissolved materials. In addition, the intercept of the fitting curve and Y-axis rose with the elevated concentration of the compound working fluid, indicating that with an increasing concentration of compound working fluid, the electrolyte conductivity and the dissolution volume were improved.

Compared to that of regular electrolytes, the electrical conductivity of the compound working fluid was relatively low. In order to eliminate the remaining recast layer (about 10 μm in thickness) after three-pass WEDM, the wire feed rate might need further reduction while using the low-concentration electrolyte, which would considerably reduce the efficiency of WECM finishing making it necessary to increase the electrolyte concentration to promote the electrochemical reaction. Although the increasing electrolyte concentration aggravated deviation, the actual dissolution volume was still linearly related to the theoretical value. Therefore, a sufficiently high-concentration electrolyte should be utilized for WECM finishing so as to remove the recast layer.

4 Results and discussion

Based on the above analysis of the model, the electrolyte conductivity is relatively slight when the concentration of compound working fluid is low. To sufficiently dissolve the recast layer, a considerably low wire feed rate is required to perform WECM finishing. To improve the finishing efficiency, the

compound working fluid with a concentration of 1:5 is utilized to perform WECM. The reverse offset of the wire electrode after three-pass WEDM is 0.030 mm. As mentioned before, the remaining recast layer that needing dissolution after three-pass WEDM is about 10 µm in thickness. Taking 10 µm as the actual dissolution volume, the corresponding theoretical value can be calculated according to the fitting result. Afterward, the desired wire feed rate for electrolysis can be calculated according to the WECM model. As shown in Fig. 7, the wire feed rate for WECM after three-pass WEDM should be set to 10 µm/s at the electrolyte concentration of 1:5. The detailed experimental parameters of the combined multi-pass WEDM and WECM are shown in Table 5.

Table 5: Optimized machining parameters for three-pass WEDM

Wire pass	Pulse width (µs)	Duty ratio	Current (A)	Wire traveling speed (m/s)	Offset (mm)	Wire feed rate (µm/s)
MC	40	1:5	4	12.0	0.000	50
TC1	10	1:8	2	7.2	+0.040	100
TC2	3	1:10	1	4.8	+0.020	80
WECM	10	1:6	0.3	2.4	-0.030	10

4.1 Surface topography and roughness

The Quattro S scanning electron microscope (SEM) from Thermo Fisher was used to investigate the machined surface topography. The VK-X1100 confocal laser scanning microscope from Keyence was used to collect 3D views and profiles then measure surface roughness of machined surface. The VK-X1100 profilemeter is a laser microscope which can measure roughness with nanometer resolution. The average surface roughness Ra was determined based on five measurements.

Fig. 9 shows the SEM micrographs and the corresponding 3D profiles of generated surfaces. As seen in Fig. 9a and 9b, the WEDM surfaces are formed by the overlaps of a multitude of stochastically distributed craters. Rapidly cooled by the dielectric fluid, the materials heated to the point of a molten state but not hot enough to be ejected into the gap and flushed away are re-solidified in the cavity, forming coral reef micro-structures. In addition, a portion of the molten debris can be re-solidified and redeposit on the machined surface before being flushed out of the gap, forming randomly-distributed spherical particles. During main cutting, higher discharge energy tends to leave larger and deeper craters on the machined surface. The thermal energy transferred to the base material increases, and thus more materials are melted, which, in turn, enhances the fraction of melted materials and unexpelled debris remaining on the surface. Therefore, the surface after the main cutting is significantly rough. As the discharge energy decreases during trim cutting, a smaller and shallower crater on the surface will be produced. Furthermore, less thermal energy is transferred to the base material decreases, and thus less material

will be melted. The re-solidified particles left on the surface are significantly reduced. The peak-to-valley height is drastically reduced from 86.26 µm to 55.45 µm. Consequently, the surface after two trim cutting gets smoother. Although the surface finish and quality can be improved after trim cutting, visible micro craters and globules can still be observed on the surface, which is attributed to the challenges of successive trim cutting to eliminate the large, deep, and randomly distributed craters generated during the main cutting. Moreover, trim cutting remains a thermal erosion process in nature, making it inevitable to form the crater and recast layer. As can be seen in Fig. 9c, the machined surface after WECM finishing is relatively lustrous, and no trace of discharge craters or redeposited materials is found on the surface, indicating the sufficient dissolution of unwanted materials. For this reason, the uniformity and flatness of the surface are significantly improved.

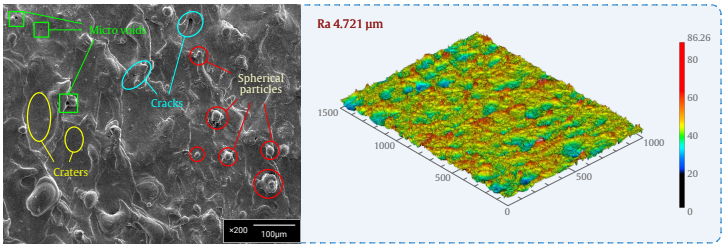

(a) Main cutting

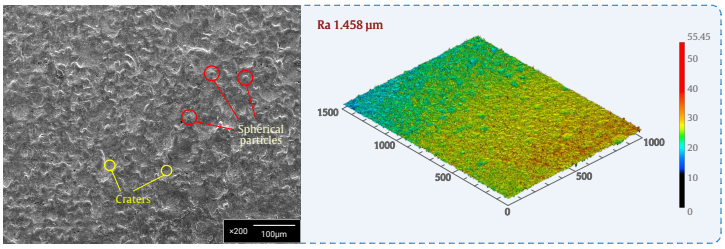

(b) Two trim cutting

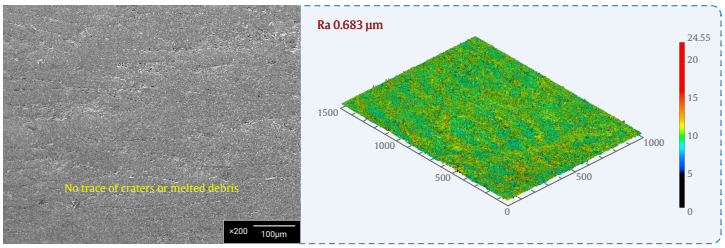

(c) WECM

Fig. 9: SEM micrographs of recast layer

4.2 Recast layer

Each specimen was ultrosonically cleaned for 2 minutes and polished to expose a cross-section of the recast layer. To reveal the recast layer, the prepared specimens were immersed in an etchant composed of 2 ml HNO_3 and 98 ml ethanol for 20 seconds. Fig. 10 shows the transverse view of the recast layer after main cutting, two trim cutting, and WECM finishing. Fig. 10a reveals the discontinuous distribution and non-uniform thickness of the recast layer after the main cutting. The average recast layer thickness is approximately 22 µm and is reduced to about 10 µm after two trim cutting, as shown in Fig. 10b. Compared to that after the main cutting, the recast layer after two trim cutting represents a significantly reduced thickness and greatly improved uniformity in distribution. Fig. 10c presents no trace of the recast layer on the surface after WECM finishing, indicating that WECM finishing based on the multi-pass WEDM is feasible to eliminate the recast layer, thus improving the surface quality.

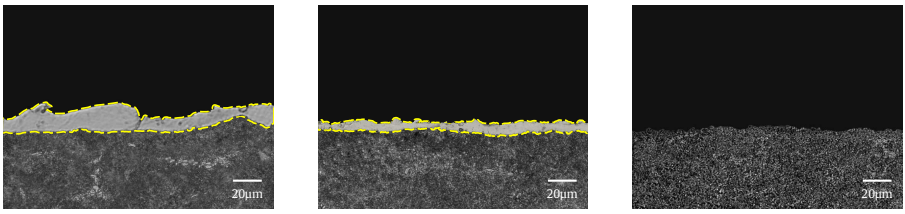

(a) Main cutting (b) Two trim cutting (c) WECM

Fig. 10: SEM micrographs of recast layer

4.3 Microhardness

Nano-indentation hardness testing was ultilized to measure the hardness of the recast layer. The iNano nanoindenter from KLA with a 50-mN load cell was utilized. The obtained depth profiles of microhardness in the machined surfaces are shown in Fig. 11. The bulk regions of the specimens were tested first, with an average hardness of 6.92 GPa. The bulk material hardness is indicated using lateral dotted line. It can be seen that the trends of the depth profile in main cutting and two trim cutting are similar. The recast layer is densely infiltrated with carbon to the point that its structure is distinctly different from that of the bulk material. The hardness of the recast layer is higher than that of the bulk material due to the rapid quenching. Beneath the recast layer is the heat-affected zone (HAZ), which is minimally affected by the carbon enrichment of the recast layer and is heated but not to the point of melting temperature. At this point, the hardness of HAZ is slightly lower than that of the bulk material. The difference in microhardness between main cutting and two trim cutting lies in the varying thicknesses of the recast

layer. As mentioned above, the surface after main cutting is overlapped with large and deep craters, with loose micro-structure like microvoids, resulting in a lower hardness in the outmost layer than in the bulk material. During WECM finishing, the loose exterior micro-structure and the recast layer are removed completely, and the remaining HAZ exhibits lower hardness than the bulk material.

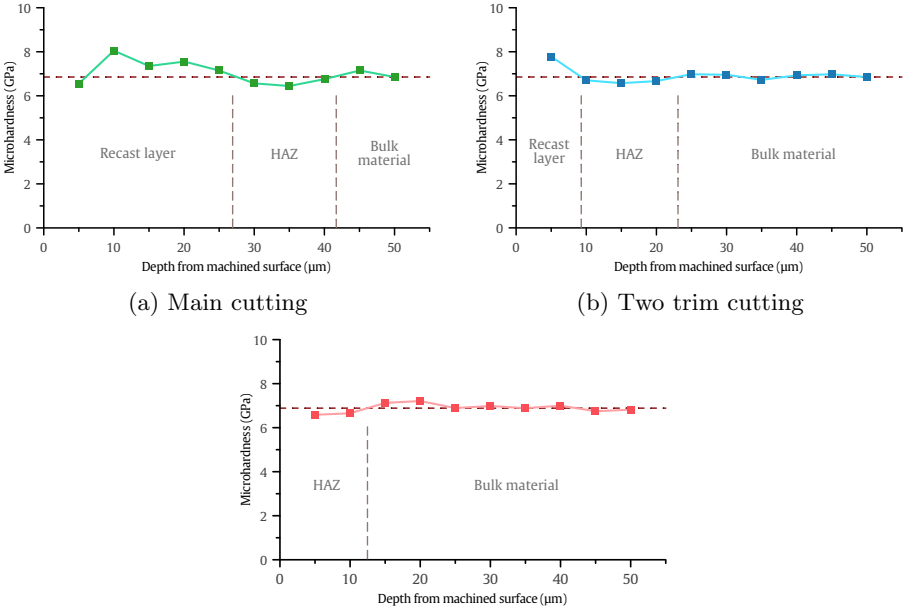

(a) Main cutting

(b) Two trim cutting

(c) WECM

Fig. 11: Dissolution volume at different concentrations of compound working fluid

5 Conclusions

The compound working fluid widely used in HSWEDM is featured by sufficient dielectric strength and slight conductivity. Based on that, this study initiates and investigates a combined WEDM and WECM machining process on the same machine tool. According to the double layer and Faraday's law of electrolysis, a theoretical model of identifying the wire feed rate during WECM finishing is established. In addition, the theoretical model is optimized by performing the combined machining at different concentrations of the compound working fluid. The following conclusions can be drawn:

1. WECM finishing after multi-pass WEDM is feasible on the same machine tool by using the compound working fluid as a bi-characteristic fluid.

2. The actual dissolution volume tends to be less than the theoretical value owing to the protective behavior of the adsorption film. As the concentration of compound working fluid increases, the protective effect of the film enhances as well, resulting in a larger deviation between the actual and theoretical dissolution volume.
3. At the consistent electrolyte concentration, the actual dissolution volume is linearly correlated to the theoretical value. Therefore, the corresponding wire feed rate for WECM finishing can be calculated by the linear fitting result according to the specific thickness of the removed recast layer.
4. After performing a three-passes WEDM with the compound working fluid concentration of 1:5, the recast layer about 10 µm thick can be removed completely at a wire feed rate of 10 µm/s. The machined surface roughness is improved to 0.683 µm Ra after WECM finishing.

Declarations

Acknowledgements. The authors extend their sincere thanks to those who contributed in the preparation of the instructions.

Author contribution. All authors have been personally and actively involved in substantive work leading to the report.

Funding. This work was supported by the National Natural Science Foundation of China (grant number 51975290).

Materials availability. The data and materials set supporting the results are included within the article.

Conflict of interest. The authors have no relevant financial or nonfinancial interests to disclose.

References

[1] Ho K, Newman S, Rahimifard S, et al (2004) State of the art in wire electrical discharge machining (WEDM). Int J Mach Tools Manuf 44(12-13):1247–1259. https://doi.org/10.1016/j.ijmachtools.2004.04.017

[2] Prasad D, Krishna AG (2015) Empirical modeling and optimization of kerf and wire wear ratio in wire electrical discharge machining. Int J Adv Manuf Technol 77(1):427–441. https://doi.org/10.1007/s00170-014-6445-8

[3] Antar M, Soo S, Aspinwall D, et al (2012) Fatigue response of Udimet 720 following minimum damage wire electrical discharge machining. Mater Des 42:295–300. https://doi.org/10.1016/j.matdes.2012.06.003

[4] Kumar S, Verma A (2021) Surface modification during electrical discharge machining process–a review. Mater Today: Proc 46:5228–5232. https://doi.org/10.1016/j.matpr.2020.08.596

[5] Ayesta I, Izquierdo B, Flano O, et al (2016) Influence of the WEDM process on the fatigue behavior of Inconel® 718. Int J Fatigue 92:220–233. https://doi.org/10.1016/j.ijfatigue.2016.07.011

[6] Singh MA, Sarma DK, Hanzel O, et al (2018) Surface characteristics enhancement of MWCNT alumina composites using multi-pass WEDM process. J Eur Ceram Soc 38(11):4035–4042. https://doi.org/10.1016/j.jeurceramsoc.2018.04.062

[7] Sharma V, Patel DS, Agrawal V, et al (2021) Investigations into machining accuracy and quality in wire electrochemical micromachining under sinusoidal and triangular voltage pulse condition. J Manuf Processes 62:348–367. https://doi.org/10.1016/j.jmapro.2020.12.010

[8] Kurita T, Hattori M (2006) A study of EDM and ECM/ECM-lapping complex machining technology. Int J Mach Tools Manuf 46(14):1804–1810. https://doi.org/10.1016/j.ijmachtools.2005.11.009

[9] Nguyen MD, Rahman M, San Wong Y (2012) Simultaneous micro-EDM and micro-ECM in low-resistivity deionized water. Int J Mach Tools Manuf 54:55–65. https://doi.org/10.1016/j.ijmachtools.2011.11.005

[10] Li L, Wei X, Li Z (2014) Surface integrity evolution and machining efficiency analysis of W-EDM of nickel-based alloy. Appl Surf Sci 313:138–143. https://doi.org/10.1016/j.apsusc.2014.05.165

[11] Mandal A, Dixit AR, Chattopadhyaya S, et al (2017) Improvement of surface integrity of Nimonic C 263 super alloy produced by WEDM through various post-processing techniques. Int J Adv Manuf Technol 93(1):433–443. https://doi.org/10.1007/s00170-017-9993-x

[12] Wu X, Li S, Jia Z, et al (2019) Using WECM to remove the recast layer and reduce the surface roughness of WEDM surface. J Mater Process Technol 268:140–148. https://doi.org/10.1016/j.jmatprotec.2019.01.016

[13] Debnath S, Kundu J, Bhattacharyya B (2018) Modeling and influence of voltage and duty ratio on wire feed in WECM: possible alternative of WEDM. J Electrochem Soc 165(2):E35. https://doi.org/10.1149/2.0601802jes

[14] Kang J, Wen J, Jayaram SH, et al (2014) Development of an equivalent circuit model for electrochemical double layer capacitors (EDLCs) with distinct electrolytes. Electrochimica Acta 115:587–598. https://doi.org/

10.1016/j.electacta.2013.11.002

[15] Pan H, Liu Z, Li C, et al (2017) Enhanced debris expelling in high-speed wire electrical discharge machining. Int J Adv Manuf Technol 93(5):2913–2920. https://doi.org/10.1007/s00170-017-0716-0